Molecular Genetics & Genomic Medicine

WILEY

Molecular Genetics & Genomic Medicine
Open Access

CLINICAL REPORT OPEN ACCESS

A Case Report of Shwachman-Diamond Syndrome Caused by Heterozygous Variants in the *EFL1* Gene and Literature Review

Xiaoying Zhou[1] | Hongxin Li[2] | Xinyi Yang[1] | Chunli Wang[3] | Wenting Zhang[1,4]

[1]Central Laboratory of Pediatrics, Affiliated Changzhou Children's Hospital of Nantong University, Changzhou, People's Republic of China | [2]Department of Neonatology, Affiliated Changzhou Children's Hospital of Nantong University, Changzhou, People's Republic of China | [3]Key Laboratory of Pediatrics, Children's Hospital of Nanjing Medical University, Nanjing, People's Republic of China | [4]Pharmaceutical Research Laboratory, Changzhou Institute of Bronchitis, Changzhou, People's Republic of China

Correspondence: Wenting Zhang (wenting_zhang@ntu.edu.cn)

Received: 29 June 2025 | **Revised:** 11 May 2026 | **Accepted:** 3 June 2026

Keywords: genetic testing | neonatal genetic disorders | Shwachman-Diamond syndrome

ABSTRACT

Objective: This investigation reports on a Shwachman-Diamond syndrome (SDS) case arising from compound heterozygous genetic variations affecting the *EFL1* locus. A systematic review of published literature was undertaken to compile data on clinical manifestations, management strategies, and prognostic indicators in SDS cases with identified *EFL1* genetic alterations.

Methods: The clinical data of a neonatal SDS patient, whole exome sequencing (WES) results, and the pathogenicity of the variants were analyzed. A comprehensive survey of applicable medical literature published up to March 2025 was executed to identify and synthesize the clinical phenotypes associated with this condition.

Results: WES identified compound heterozygous variants within the patient's *EFL1* gene: c.2935C>T (p.R979C) and c.3149_3151delCAC (p.P1050del). Bioinformatics analysis indicated these variations were damaging. Seven articles reported a total of 20 cases of this disease, with predominant phenotypes including exocrine pancreatic insufficiency, hematologic abnormalities, and metaphyseal dysplasia. Among the 20 previously reported cases, 16 distinct EFL1 variants were identified, and the current case adds 2 novel variants.

Conclusion: SDS caused by *EFL1* gene defects primarily presents as bone marrow failure, with treatment mainly focused on symptomatic management. We report a neonatal SDS patient with the earliest onset of symptoms. The c.2935C>T and c.3149_3151delCAC compound heterozygous variants reported in this study expand the mutational spectrum of this disease.

1 | Introduction

Shwachman-Diamond syndrome (SDS) (OMIM #260400) is a rare autosomal recessive ribosomal disorder characterized by prominent clinical manifestations, including hematopoietic dysfunction, pancreatic exocrine insufficiency, and skeletal abnormalities. Additionally, patients exhibit a significant predisposition to bone marrow failure and myelodysplastic syndrome, with approximately 10%–30% of cases developing myeloid malignancies (Donadieu et al. 2012; Furutani et al. 2022; Myers et al. 2020). The pathogenesis of SDS is attributed to genetic defects that impair ribosome maturation (Finch et al. 2011; Menne et al. 2007). Recent studies have shown that variations in the *SBDS*, *EFL1*, *DNAJC21*, and *SRP54* genes can lead to this disease. A common feature among these genes is their involvement in the generation, assembly, and function of ribosomal proteins. Among these, approximately 90% of SDS cases harbor variations in the *SBDS*

gene (Boocock et al. 2003). Defects in the *SRP54* gene have been shown to give rise to an SDS-like phenotype, whereas defects in the *DNAJC21* gene may be associated with type 3 bone marrow failure syndrome (Bellanne-Chantelot et al. 2018; Carapito et al. 2017; Tummala et al. 2016). Variations in the *EFL1* gene specifically impair the assembly of the 80S ribosome, thereby contributing to the development of SDS (Finch et al. 2011; Menne et al. 2007; Tan et al. 2019). To date, the Human Genome Mutation Database (HGMD) has recorded only 17 EFL1 variations (https://www.hgmd.cf.ac.uk/ac/gene.php?gene=EFL1), most of which are missense variations.

In this study, we report a novel case of SDS in a Chinese neonatal patient harboring compound heterozygous variants in the *EFL1* gene: c.2935C>T (p.R979C) and c.3149_3151delCAC (p.P1050del). Both variants are previously unreported, significantly expanding the known mutational spectrum of the *EFL1* gene. Notably, our patient exhibited the earliest documented onset of symptoms (6-day-old), providing novel clinical insights into the neonatal presentation of this rare disorder. Furthermore, we review the existing literature to enhance the clinical recognition and diagnostic precision of *EFL1*-associated SDS for pediatric clinicians.

2 | Subjects and Methods

2.1 | Subjects

A 6-day-old female neonate was admitted to the Department of Neonatology, Affiliated Changzhou Children's Hospital of Nantong University, in October 2024, hospitalized with a diagnosis of "post-natal thrombocytopenia persisting for 6 days". The infant was delivered from a primigravida mother at 37 weeks gestation, weighing 1780 g at birth (falling below the 3rd percentile for gestational age), classified as a small-for-gestational-age infant. She was delivered vaginally at a local obstetrics and gynecology hospital with clear amniotic fluid and a coiled umbilical cord. At 1 min after birth, the infant's Apgar assessment yielded a score of 1, which subsequently improved to 10 when re-evaluated at the 5-min mark. During hospitalization, thrombocytopenia and coagulation abnormalities were detected. Despite the administration of plasma, prothrombin complex, and fibrinogen, no improvement was observed, and she was transferred to our hospital. On admission, her weight was 1750 g. Physical examination revealed mild jaundice with no signs of bruising or petechiae. Laboratory results at admission showed platelet count of 12×10^9/L, white blood cell count of 7.36×10^9/L, neutrophil count of 2.1×10^9/L, coagulation profile with activated partial thromboplastin time (APTT) of 42.0 s, and D-dimer of 34.71 mg/L. Following treatment with plasma transfusion, hemoglobin, vitamin K1, and antibiotics, the platelet count gradually increased to 395×10^9/L, and neutrophil and white blood cell counts did not show significant reductions. The D-dimer decreased to 0.23 mg/L, but APTT remained elevated at 57.6 s. By one month of age, her weight had increased to 2.31 kg. The parents were healthy, and there was no family history of similar conditions. Given the persistent coagulation abnormalities and growth restriction, genetic testing was recommended to the parents.

At 8 months of age, her height was 64 cm and weight was 6 kg, both below the 3rd percentile for age. At the latest follow-up, the patient is 18 months of age and demonstrates global growth and developmental delay. She achieved head control at 6 months of age but is currently unable to roll over or sit independently and exhibits poor suckling with consequent feeding difficulties. No skeletal abnormalities or exocrine pancreatic insufficiency have been observed to date. Fecal elastase testing was not performed; serum amylase levels were within normal limits. Bone marrow examination was not undertaken during the course of illness, as the family declined the procedure despite our recommendation. Serum vitamin A level was 0.690 μmol/L (reference range: 0.52–2.2 μmol/L) and vitamin E level was 10.925 μg/mL (reference range: 10–15 μg/mL), both within normal limits. Vitamin K levels were not assessed. Hepatic ultrasonography revealed no significant abnormalities. Platelet counts normalized at the time of discharge, and subsequent monthly complete blood count monitoring over the following 6 months demonstrated no recurrent thrombocytopenia; the surveillance interval was thereafter extended to once every 3 months.

2.2 | Methods

2.2.1 | Genetic Sequencing

Parental authorization was secured prior to extracting 3 mL of peripheral blood from the child patient and parents. Following the manufacturer's protocol, genomic DNA was isolated from blood samples utilizing the Tiangen Blood Genomic DNA Extraction Kit (DP318). The DNA samples were sent to Beijing Chigene Translational Medical Research Center for whole exome sequencing (WES). The patient's guardian provided signed informed consent before blood sampling commenced. The study protocol received approval from Changzhou Children's Hospital's Medical Ethics Committee (No. 2023-002).

2.2.2 | Sanger Sequencing

Sanger sequencing validation for the detected pathogenic variants reported in WES was performed. Primer 5.0 software was used to design primers for the candidate variants; the primer sequences were shown in Table 1. Amplification conditions: predenaturation at 96°C for 2 min, denaturation at 96°C for 30 s, annealing at 60°C for 30 s, extension at 72°C for 45 s, cycling 30 times, and final extension at 72°C for 5 min.

2.2.3 | Bioinformatics Analysis

The paired-end reads were aligned to the Ensembl GRCh37/hg19 human reference genome using the Burrows-Wheeler Aligner (BWA) software (Li and Durbin 2010). Subsequently, single nucleotide variants (SNVs) and small insertions/deletions (InDels) were called using the Genomic Analysis Toolkit (GATK) software (version 4.1.7) (McKenna et al. 2010). The genetic relationship was determined by KING (Manichaikul et al. 2010), and the coverage of the SRY gene was calculated through gender quality control. The identified variants were then annotated utilizing an online system developed by Chigene (www.chigene.org), which incorporates

a comprehensive set of 35 public databases. For minor allele frequency annotation, databases such as 1000 genomes, dbSNP, ESP, ExAC, and Chigene's in-house MAFs database were employed. To predict structural variations in protein products caused by these variants, Provean, Sift, PolyPhen2_hdiv, PolyPhen2_hvar, Mutationtaster, M-Cap, and Revel software packages were utilized. Additionally, the functional impact on splicing sites was predicted using MaxEntScan, dbscSNV, and SpliceAI software packages, and the ACMG/AMP variant classification guidelines were employed for variant classification (Richards et al. 2015; Riggs et al. 2020). Conservation analysis of the variants was performed using Consurf (https://consurf.tau.ac.il/consurf_index.php). The specific impact of the variants on SR protein binding was analyzed using ESE Finder 3.0 (http://rulai.cshl.edu/cgi-bin/tools/ESE3/esefinder.cgi), with threshold values set at SF2/ASF: 1.956, SC35: 2.383, SRp40: 2.67, and SRp55: 2.676. Candidate SNVs were confirmed by Sanger sequencing. The wild-type tertiary structure of the EFL1 protein was retrieved from the AlphaFold Protein Structure Database (Identifier: AF-Q7Z2Z2-F1). To evaluate the structural impact of the identified p.1050del variant, a 3D mutant model was generated via homology modeling using the Swiss-Model server (https://swissmodel.expasy.org/). Structural visualizations and comparative analyses of hydrogen bonding interactions were performed using PyMOL software (v2.5).

2.2.4 | Literature Review

Given the limited reports of EFL1-related SDS, we thoroughly reviewed the cases published in PubMed.

3 | Results

3.1 | Genetic Sequencing Results

The WES identified two compound heterozygous variants in the *EFL1* gene (Transcript: NM_024580.6): a missense variation *c.2935C>T* (p.R979C) and a non-frameshift deletion *c.3149_3151delCAC* (p.P1050del). Subsequent Sanger sequencing confirmed that these two pathogenic variations were inherited from the parents, with *c.2935C>T* inherited from the father and *c.3149_3151delCAC* inherited from the mother (Figure 1).

3.2 | Pathogenicity Analysis of Variants

According to the ACMG variant classification guidelines, the c.2935C>T (p.R979C) (PM2_Supporting + PP3) and c.3149_3151delCAC (p.P1050del) (PM2_Supporting + PM4)

TABLE 1 | Primer sequences for Sanger sequencing verification of EFL2 gene. c.3149_3151delCAC and c.2935C>T variants.

Primer	Sequence 5′ → 3′	Annealing temperature (°C)	Fragment size (bp)
EFL1-Exon19F	GCTACTCTTGGCCTCCTCTGTAGG	60	714
EFL1-Exon19R	GCCAGTTGCTTGCCTACTAAGCC		
EFL1-Exon18F	TTCACTGTTATTCAGGGCATTTCT	60	577
EFL1-Exon18R	CCAAATCTGGTCATTTGGCCC		

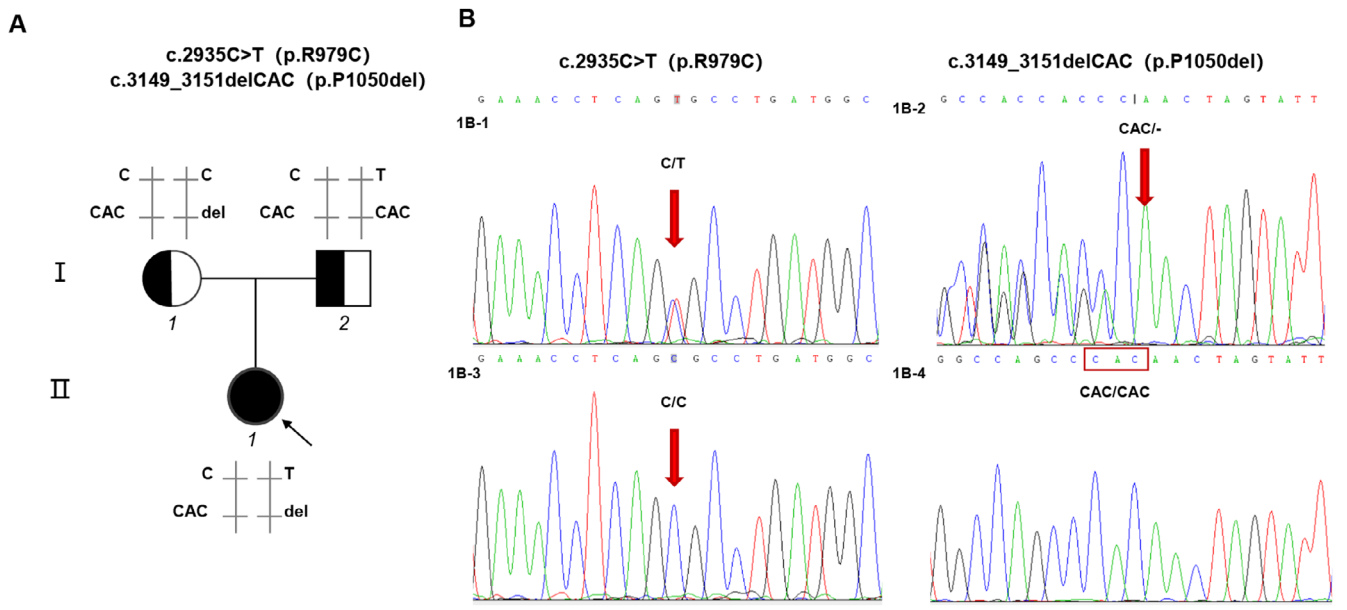

FIGURE 1 | The family harbored *EFL1* variants identified by WES and Sanger analysis. (A) The pedigree of this patient's family, with II-1 indicating the proband (the patient). The patient inherited the EFL1 variants of c.2935C>T from the father (I-2) and c.3149_3151delCAC from the mother (I-1). (B) The Sanger sequencing of the *EFL1* gene in this family, where 1B-1 and 1B-2 represent the mutant type, while 1B-3 and 1B-4 represent the wild type.

variants were classified as variants of uncertain significance. These two variants were not recorded in the ClinVar, HGMD, or OMIM databases, and both were not detected in normal population databases, indicating that they are rare variants.

The c.2935C>T variant causes an arginine at position 979 to be substituted by cysteine. Analysis using Mutation Taster, Revel score, PolyPhen2, and SIFT indicated that this variant is pathogenic (Table 2). Conservation analysis using Consurf revealed that this site is highly conserved (Figure 2A). The variant is located in domain IV (Figure 2B). The *EFL1* domain IV can interact with its cofactor *SBDS* domains II/III, thereby forming a low-affinity binding mode on the ribosome (Figure 2D; Weis et al. 2015). This suggests that variations at this site may disrupt the protein's interaction with *SBDS*, potentially affecting ribosome assembly.

The c.3149_3151delCAC variant leads to a deletion of proline at position 1050, resulting in a change in protein length. Analysis using Mutation Taster indicated that this variant is pathogenic (Table 2). The results of evolutionary conservation assessment performed via Consurf indicate that the amino acid residue missing at position 1050 maintains high conservation throughout evolutionary history (Figure 2A). Further prediction using ESE Finder 3.0 suggested that this variant would disrupt exonic splicing enhancer (ESE) motifs that bind two SF2/ASF, one SC35, and one SRp40, and that the variation would form a new ESE motif that binds SF2/ASF (Figure 2C). Thus, it is hypothesized that this variant may affect the splicing of the *EFL1* gene precursor mRNA. The variant is located in domain V (Figure 2B). This domain facilitates the repositioning of *SBDS* around helix 69, and it is likely that this variation disrupts the proper repositioning of *SBDS*, thus impairing ribosomal function (Weis et al. 2015; Figure 2D).

Based on the clinical manifestations, genetic testing results, and pathogenicity analysis of the variants, a diagnosis of SDS was established for this patient at 1 month of age.

3.3 | Literature Review

Given the limited reports of *EFL1*-related SDS, we thoroughly reviewed the cases published in PubMed for articles published up until March 2025. No relevant Chinese articles were found. To date, seven English language articles have reported 20 cases

TABLE 2 | Bioinformatics analysis for predicting the functional effects of c.2935C>T and c.3149_3151delCAC in FEL-1.

Variants	Mutation testing	Revel score	PolyPhen2	SIFT
c.2935C>T	Disease causing	0.599 (deleterious)	1.0 (probably damaging)	0.0 (damaging)
c.3149_3151delCAC	Disease causing	—	—	—

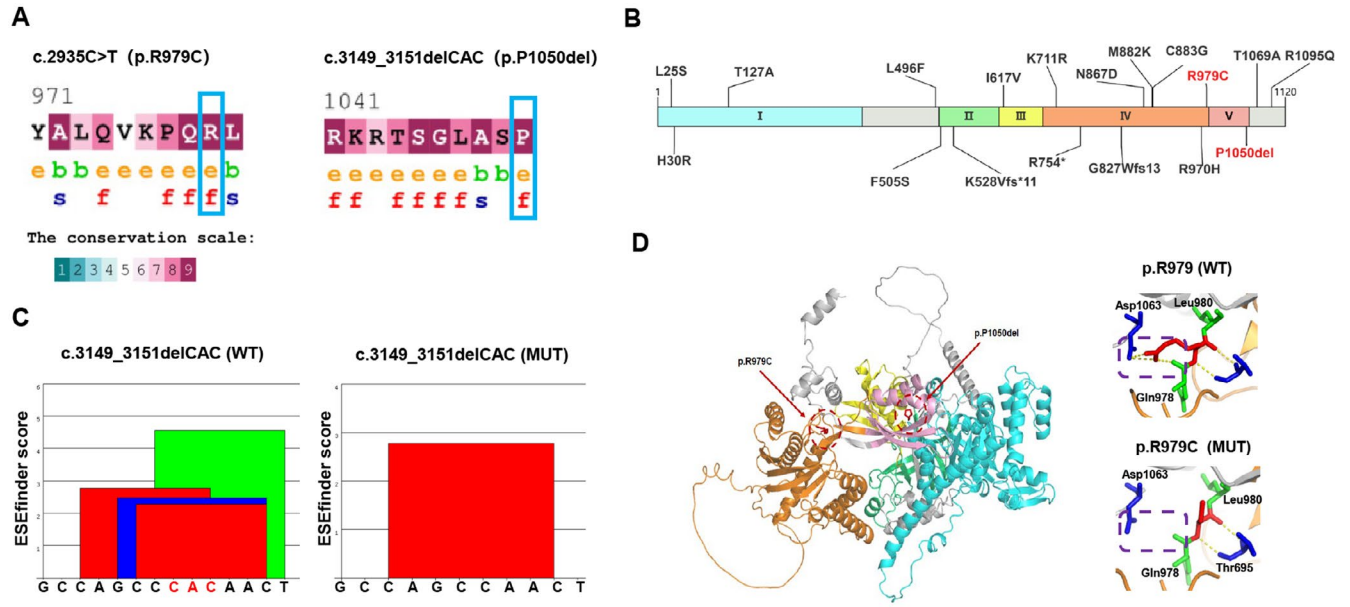

FIGURE 2 | The bioinformatics analysis of c.2935C>T and c.3149_3151delCAC. (A) Consurf conservation analysis of c.2935C>T and c.3149_3151delCAC, with deeper purple indicating higher conservation. The blue box highlights the mutation sites. (B) Locations of 18 different EFL1 allelic mutations in the secondary structure. The two variants (c.2935C>T and c.3149_3151delCAC) carried by the patient in this case are marked in red. (C) ESE Finder 3.0 predicts that c.3149_3151delCAC disrupts ESE motifs binding to 2 SF2/ASF, 1 SC35, and 1 SRp40, while forming a new SF2/ASF-binding ESE motif post-mutation. (D) Positions of c.2935C>T and c.3149_3151delCAC in the tertiary structure of the EFL1 protein. The wild-type structure was obtained from the AlphaFold database (AF-Q7Z2Z2-F1). Structural visualizations and comparative analyses of hydrogen bonding interactions were performed using PyMOL software (v2.5). In the left panel, the five structural domains of EFL1 are color-coded as follows: Domain I (blue), II (green), III (yellow), IV (orange), and V (pink). In the right panel, the wild-type (WT, up) and the p.R979C mutant (MUT, down) structures are presented to highlight local conformational and hydrogen-bonding differences caused by the variant. Red indicates the mutated amino acids (AA), blue shows hydrogen-bonded residues, green marks residues adjacent to the mutated AA, yellow dashed lines indicate hydrogen bonds; and the purple box highlights the site of hydrogen bond loss caused by the c.2935C>T variation.

TABLE 3 | Reported *EFL1* variants causing SDS.

No.	Mutation	Gender	Clinical manifestation				Prognosis (age at report)
			Hematology	Gastroenterology	Skeleta	Other	
1	*c.2645 T>A*/p. Met882Lys(hom)	M	Hematologic system: chronic neutropenia, transient anemia, and thrombocytopenia. Bone marrow examination normal	Neonatal period: feeding difficulties. 2 years: pancreatic insufficiency with intermittent diarrhea and constipation.	7 months: metaphyseal dysplasia (ribs and femurs).	Short stature, developmental delay. Neonatal period: hypotonia, subglottic stenosis, laryngocele, laryngeal softening, umbilical hernia Later, frequent infections, severe myopia	Alive (6 years)
2	*c.2645 T>A*/p. Met882Lys(hom)	F	Hematologic system: intermittent neutropenia. Bone marrow examination normal.	Pancreatic insufficiency.	Metaphyseal dysplasia (ribs and femurs)	Short stature, severe myopia, mild speech delay, short stature	Alive (4 years)
3	*c.3284G>A*/p. Arg1095Gln(hom)	F	Hematologic system: progressive severe neutropenia, progressive anemia, and fluctuating thrombocytopenia. Bone marrow examination: pancytopenia.	Pancreatic insufficiency with severe diarrhea and fat malabsorption.	Metaphyseal dysplasia (ribs and limbs).	Low birth weight, hypotonia, microcephaly, low-set ears, high-arched palate, shortened limbs and fingers. Poor growth and development.	Died at 14 months
4	*c.3284G>A*/p. Arg1095Gln(hom)	M	Clinical manifestations similar to patient 3.				Died at 15 months
5	*c.3284G>A*/p. Arg1095Gln(hom)	M	Clinical manifestations similar to patient 3, symptoms relieved after enzyme replacement therapy.				Alive (15 months)
6	*c.3284G>A*/p. Arg1095Gln(hom)	F	Clinical manifestations similar to patient 3.				Died at 7 months
7	*c.379A>G*/p.Thr127Ala(hom)	F	Mild neonatal thrombocytopenia. Hematologic system: mild and intermittent thrombocytopenia, no anemia or neutropenia. Bone marrow examination: pancytopenia.	Liver disease from 2 to 4 years old. No gastrointestinal symptoms, with mild exocrine pancreatic insufficiency.	Metaphyseal dysplasia of limbs and vertebral bodies. Scoliosis with restrictive lung disease.	SGA. Developmental delay.	Alive (14 years)

(Continues)

TABLE 3 | (Continued)

No.	Mutation	Gender	Clinical manifestation				Prognosis (age at report)
			Hematology	Gastroenterology	Skeleta	Other	
8	*c.2260C>T*/p.Arg754*; *c.1514 T>C*/p.Phe505Ser	M	Hematologic system: at age 17, mild thrombocytopenia, progressive neutropenia, and mild anemia. Bone marrow examination: decreased cellularity and reduced segmentation of neutrophils.	At age 27: chronic diarrhea and pancreatic insufficiency, cirrhosis.	At age 5: unsteady gait, spontaneous fractures, and genu valgum. At age 13: metaphyseal chondrodysplasia.	SGA. Mild intellectual disability.	Alive (31 years)
9	c.2908C>T/p.Arg970His(hom)	F	At 3.8 years: neutropenia, thrombocytopenia. Hematological system: iron-deficiency anemia, mild thrombocytopenia, and neutropenia. Bone marrow examination: reduced segmentation of central granulocytes.	At 13 months: anorexia, elevated liver enzymes. At 3.8 years: exocrine pancreatic insufficiency.		SGA. At 13 months: developmental delay, reduced vitamin levels, iron-deficiency anemia. At 1.5 years: ataxia and nystagmus. At 3.8 years: Severe myopia.	Alive (11 years)
10	c.2647T>G/p.Cys883Gly; reduced *EFL1* expression	F	Severe neonatal anemia, thrombocytopenia. Hematological system: transfusion-dependent anemia until 2 years, then improved. Bone marrow examination: erythrocyte reduction and reduced segmentation of central granulocytes.	Elevated liver enzymes. At 3 months: exocrine pancreatic insufficiency with chronic diarrhea. Anorexia.	Pectus carinatum, short limbs. At 3 months: Vertebral, limb, and rib cartilage dysplasia.	At 3 months: growth retardation. Intellectual developmental delay.	Alive (7 years)
11	*c.2478dupT*/p.Gly827Trpfs13;*c.3205A>G*/p.Thr1069Ala	M	At 2 months: pancytopenia. Hematological system: pancytopenia. Bone marrow examination: granulocytopenia, reduced megakaryopoiesis, increased iron stores.	At 2 months: Exocrine pancreatic insufficiency with lipomatosis.	At 2 months: Epiphyseal cartilage dysplasia.	Preterm, SGA.	Alive (3 years)
12	*c.89A>G*/p.His30Arg; *c.3205A>G*/p.Thr1069Ala	M	Hematological system: –; Bone marrow examination: —	Pancreatic lipomatosis	Metaphyseal dysplasia	Preterm, SGA. short stature.	Alive (9 years)

(Continues)

TABLE 3 | (Continued)

No.	Mutation	Gender	Clinical manifestation				Prognosis (age at report)
			Hematology	Gastroenterology	Skeleta	Other	
13	*c.89A>G*/p.His30Arg; *c.3205A>G*/p.Thr1069Ala	F	Hematological system: anemia, thrombocytopenia, and intermittent neutropenia from 2 years old.	At 2 years: exocrine and endocrine pancreatic insufficiency. pancreatic lipomatosis.	At 2 years: metaphyseal dysplasia. osteoporosis	SGA. ichthyosis.	Alive (25 years)
14	*c.89A>G*/p.His30Arg; *c.2599A>G*/p.Asn867Asp	F	Severe neonatal persistent pancytopenia. Hematology: severe persistent neonatal pancytopenia. Severe neutropenia and recurrent infections. Bone marrow examination: reduced cell count and reduced segmentation of central granulocytes.	At 5 months: exocrine pancreatic insufficiency, later diagnosed with endocrine dysfunction. Gastrostomy for enteral feeding.	Mild limb shortening.	Preterm, SGA. High palatal arch. Pulmonary hypertension, pulmonary insufficiency, lifelong ventilatory support, and tracheostomy. Suspected structural lung disease.	Died at 18 months.
15	*c.1581_1587delCAAATAC*/p.K528Vfs*11; *c.74T>C*/p.L25S	F	Hematological system: initially leukopenia and thrombocytopenia, later progressed to pancytopenia. Bone marrow examination: increased granulocytes and erythrocytes, increased megakaryocytes.	Long-term moderate diarrhea, malnutrition, splenomegaly, elevated liver enzymes, cirrhosis.	—	—	Alive (44 years)
16	*c.2132A>G*/p.K711R;*c.1849A>G*/p.I617V	M	Hematological system: –; Bone marrow examination: no abnormalities.	Exocrine pancreatic insufficiency.	—	Growth and developmental delay	Alive (26 years)
17	*c.2132A>G*/p.K711R;*c.1849A>G*/p.I617V	F	Hematological system: refractory thrombocytopenia, mild neutropenia. Bone marrow examination: no abnormalities.	Exocrine pancreatic insufficiency.	—	—	Alive (20 years)

(Continues)

TABLE 3 | (Continued)

No.	Mutation	Gender	Clinical manifestation				Prognosis (age at report)
			Hematology	Gastroenterology	Skeleta	Other	
18	*c.2132A>G*/p.K711R;*c.1849A>G*/p.I617V	F	Hematological system: refractory thrombocytopenia, severe neutropenia. Bone marrow examination: Lower-risk MDS.	Exocrine pancreatic insufficiency	—	Growth and developmental delay	Alive (41 years)
19	*c.2132A>G*/p.K711R;*c.1849A>G*/p.I617V	M	Hematological system: refractory thrombocytopenia, mild neutropenia. Bone marrow examination: Lower-risk MDS.	Exocrine pancreatic insufficiency	—	Growth and developmental delay.	Alive (35 years)
20	*c.1486C>T*/p.L496F(hom)	M	Hematological system: –; Bone marrow examination: Lower-risk MDS.	Exocrine pancreatic insufficiency	—	Growth and developmental delay.	Alive (24 years)

of EFL1-associated SDS, all of which are summarized in Table 3 (Cario et al. 2024; Morini et al. 2019; Stepensky et al. 2017; Tan et al. 2018; Tan et al. 2019; Zhu et al. 2024).

Among the 21 patients, the male-to-female ratio was 9:12. Four of the patients have died, and the oldest surviving patient is currently 44 years old. 20 cases reported exocrine pancreatic insufficiency, while 3 cases specifically noted pancreatic lipomatosis. Twelve patients exhibited metaphyseal dysplasia. Eight patients were small for gestational age infants (SGA) during the neonatal period. In terms of hematologic phenotypes, 17 patients had varying degrees of neutropenia, 16 patients had varying degrees of thrombocytopenia, and 8 patients developed anemia during the course of the disease. Additionally, one patient presented with liver dysfunction and cirrhosis as the main phenotype. The patient in this report primarily presented with thrombocytopenia and coagulopathy and was also diagnosed as SGA. Due to the early onset of the disease, some phenotypes have not yet manifested and will require further follow-up.

The *EFL1* gene identification results of the 21 patients were as follows: 9 cases were homozygous, and 12 cases were compound heterozygous. Mutational analysis detected 18 separate variants in *EFL1* alleles, categorized as follows: 14 missense variants, 1 nonsense variant, 2 frameshift variants, and 1 in-frame deletion. Among the 4 patients carrying the homozygous c.3284G>A/p.Arg1095Gln variations, 3 have since died, whereas the fourth survived owing to timely enzyme replacement therapy. In addition, 1 patient carrying the compound heterozygous c.89A>G/p.His30Arg and c.2599A>G/p.Asn867Asp variations has also passed away.

4 | Discussion

As an exceptionally uncommon condition, SDS occurs at a frequency of roughly 0.5–1.5 cases among every 100,000 neonates delivered alive. The median age of onset is 0.16 years, but the median age of diagnosis is 1.3 years later than the age of onset, indicating a delay in diagnosis. This highlights the need for increased awareness of the disease (Han et al. 2023). This article primarily reviews SDS caused by *EFL1* deficiency. Hematological disorders, growth deficiency, and pancreatic exocrine insufficiency represent the main clinical manifestations of this condition, corresponding to the hallmark features typically seen in SDS. However, the severity of the disease varies among affected individuals (Cario et al. 2024). The *EFL1* gene is located on chromosome 15q25.2, consists of 20 exons, and encodes the elongation factor-like GTPase 1, a protein of 1120 amino acids. The main functions of EFL1 protein are as follows: (1) It participates in the late cytoplasmic maturation of the 60S ribosomal subunit and the translational activation of ribosomes; (2) Together with SBDS, EFL1 triggers the GTP-dependent release of eIF6 from cytoplasmic pre-60S ribosomal subunits, thereby licensing 80S assembly and rendering the ribosome translation-competent; (3) The released eIF6 is recycled back to the nucleus, where it is required for 60S rRNA processing and nuclear export (Finch et al. 2011; Menne et al. 2007; Senger et al. 2001; Weis et al. 2015).

The final diagnosis of this disease relies on genetic testing. However, the *EFL1* gene has two pseudogenes (*EFL1P1* and

EFL1P2) and exhibits segmental duplications with remarkable similarity (Tan et al. 2019), making genetic testing highly challenging. Therefore, the analysis of clinical manifestations and laboratory tests is particularly important in the diagnosis of this disease. Within the documented cohort, genetic analysis revealed that a single pediatric patient harbored a paternally transmitted heterozygous variation, specifically c.2647T>G/p.C883G. Subsequent verification revealed that the child and their mother had non-coding defects in their alleles, resulting in *EFL1* gene expression defects and disease onset (Tan et al. 2019). Additionally, later literature reports suggest the presence of somatic uniparental disomy in the *EFL1* gene in hematopoietic cells, leading to a loss of heterozygosity in the neutral copy number of all or part of chromosome 15 carrying the *EFL1* locus, thus causing the disease. However, genetic testing may show only heterozygous variations (Revy and Donadieu 2021). As a result, experts recommend that patients with high suspicion of SDS who carry only heterozygous variations undergo evaluation of *EFL1* protein expression.

The main treatments for SDS include pancreatic enzyme replacement, granulocyte colony-stimulating factor, and immunosuppressive therapy. Some children with malignancies may require bone marrow transplantation (Han et al. 2023). After symptomatic treatment, the patient's platelet count returned to normal. Following clinical improvement, she was discharged.

Previous studies have suggested that patients with *EFL1* variations may exhibit a more severe clinical phenotype compared to those with *SBDS* variations (Tan et al. 2018). Our findings support this observation, as the patient demonstrated an exceptionally early onset of symptoms. However, given that our patient is currently only 18 months old, it is possible that some severe or progressive clinical manifestations may not have manifested yet, necessitating long-term and rigorous follow-up to monitor the disease progression and the long-term outcomes of symptomatic treatment.

This study reports a unique case of SDS in a Chinese neonate, characterized by the earliest documented symptom onset (6 days after birth) and the identification of two previously unreported compound heterozygous *EFL1* variants, c.2935C>T (p.R979C) and c.3149_3151delCAC (p.P1050del). This case broadens the known mutational spectrum of *EFL1* and highlights a critical clinical lesson: *EFL1*-related SDS can present with severe, early-life hematologic abnormalities even before classic pancreatic or skeletal signs manifest. The emergence of significant developmental delays at the 18-month follow-up underscores the necessity for clinicians to prioritize early genomic sequencing for rapid diagnosis in neonates with unexplained thrombocytopenia. Furthermore, it emphasizes the importance of implementing rigorous, long-term multi-disciplinary surveillance to monitor disease progression and optimize symptomatic management outcomes as the clinical phenotype evolves with age.

Author Contributions

Xiaoying Zhou and Wenting Zhang conceived this study, drafted, reviewed, and revised the manuscript. Xiaoying Zhou, Hongxin Li, and Xinyi Yang collected the clinical data and participated in the edition and revision of the manuscript. Xiaoying Zhou and Chunli Wang performed bioinformatic analysis. All authors contributed to this work and approved the submitted article.

Acknowledgements

The authors thank all the participants involved in this article.

Funding

This work was supported by Scientific Research Project of Jiangsu Health Commission (MQ2024030); Changzhou Sci&Tech Program (CJ20245049); Clinical Research Project of Nantong University (2025JZ014); Scientific Research Project of Changzhou Health Commission (QY202505).

Ethics Statement

This research protocol has been reviewed and approved by the Ethics Committee of Affiliated Changzhou Children's Hospital of Nantong University (Changzhou, China) (No. 2023-002). Written informed consent was obtained from the patient's parents in this study.

Consent

The parents of patient provided written informed consent for their personal or clinical details, along with any identifying images, to be published in this study.

Conflicts of Interest

The authors declare no conflicts of interest.

Data Availability Statement

All data relevant to the study are included in the article.

References

Bellanne-Chantelot, C., B. Schmaltz-Panneau, C. Marty, et al. 2018. "Mutations in the SRP54 Gene Cause Severe Congenital Neutropenia as Well as Shwachman-Diamond-Like Syndrome." *Blood* 132, no. 12: 1318–1331. https://doi.org/10.1182/blood-2017-12-820308.

Boocock, G. R., J. A. Morrison, M. Popovic, et al. 2003. "Mutations in SBDS Are Associated With Shwachman-Diamond Syndrome." *Nature Genetics* 33, no. 1: 97–101. https://doi.org/10.1038/ng1062.

Carapito, R., M. Konantz, C. Paillard, et al. 2017. "Mutations in Signal Recognition Particle SRP54 Cause Syndromic Neutropenia With Shwachman-Diamond-Like Features." *Journal of Clinical Investigation* 127, no. 11: 4090–4103. https://doi.org/10.1172/JCI92876.

Cario, H., A. Bertrand, S. Tan, et al. 2024. "Shwachman-Diamond Syndrome due to Biallelic EFL1 Variants With Complex and Fatal Clinical Course in Early Infancy." *British Journal of Haematology* 205, no. 6: 2363–2369. https://doi.org/10.1111/bjh.19793.

Donadieu, J., O. Fenneteau, B. Beaupain, et al. 2012. "Classification of and Risk Factors for Hematologic Complications in a French National Cohort of 102 Patients With Shwachman-Diamond Syndrome." *Haematologica* 97, no. 9: 1312–1319. https://doi.org/10.3324/haematol.2011.057489.

Finch, A. J., C. Hilcenko, N. Basse, et al. 2011. "Uncoupling of GTP Hydrolysis From eIF6 Release on the Ribosome Causes Shwachman-Diamond Syndrome." *Genes & Development* 25, no. 9: 917–929. https://doi.org/10.1101/gad.623011.

Furutani, E., S. Liu, A. Galvin, et al. 2022. "Hematologic Complications With Age in Shwachman-Diamond Syndrome." *Blood Advances* 6, no. 1: 297–306. https://doi.org/10.1182/bloodadvances.2021005539.

Han, X., S. Lu, C. Gu, Z. Bian, X. Xie, and X. Qiao. 2023. "Clinical Features, Epidemiology, and Treatment of Shwachman-Diamond Syndrome: A Systematic Review." *BMC Pediatrics* 23, no. 1: 503. https://doi.org/10.1186/s12887-023-04324-3.

Li, H., and R. Durbin. 2010. "Fast and Accurate Long-Read Alignment With Burrows-Wheeler Transform." *Bioinformatics* 26, no. 5: 589–595. https://doi.org/10.1093/bioinformatics/btp698.

Manichaikul, A., J. C. Mychaleckyj, S. S. Rich, K. Daly, M. Sale, and W. M. Chen. 2010. "Robust Relationship Inference in Genome-Wide Association Studies." *Bioinformatics* 26, no. 22: 2867–2873. https://doi.org/10.1093/bioinformatics/btq559.

McKenna, A., M. Hanna, E. Banks, et al. 2010. "The Genome Analysis Toolkit: A MapReduce Framework for Analyzing Next-Generation DNA Sequencing Data." *Genome Research* 20, no. 9: 1297–1303. https://doi.org/10.1101/gr.107524.110.

Menne, T. F., B. Goyenechea, N. Sanchez-Puig, et al. 2007. "The Shwachman-Bodian-Diamond Syndrome Protein Mediates Translational Activation of Ribosomes in Yeast." *Nature Genetics* 39, no. 4: 486–495. https://doi.org/10.1038/ng1994.

Morini, J., L. Nacci, G. Babini, et al. 2019. "Whole Exome Sequencing Discloses Heterozygous Variants in the DNAJC21 and EFL1 Genes but Not in SRP54 in 6 Out of 16 Patients With Shwachman-Diamond Syndrome Carrying Biallelic SBDS Mutations." *British Journal of Haematology* 185, no. 3: 627–630. https://doi.org/10.1111/bjh.15594.

Myers, K. C., E. Furutani, E. Weller, et al. 2020. "Clinical Features and Outcomes of Patients With Shwachman-Diamond Syndrome and Myelodysplastic Syndrome or Acute Myeloid Leukaemia: A Multicentre, Retrospective, Cohort Study." *Lancet Haematology* 7, no. 3: e238–e246. https://doi.org/10.1016/S2352-3026(19)30206-6.

Revy, P., and J. Donadieu. 2021. "EFL1 Deficiency: A Little Is Better Than Nothing." *Blood* 138, no. 21: 2016–2018. https://doi.org/10.1182/blood.2021012724.

Richards, S., N. Aziz, S. Bale, et al. 2015. "Standards and Guidelines for the Interpretation of Sequence Variants: A Joint Consensus Recommendation of the American College of Medical Genetics and Genomics and the Association for Molecular Pathology." *Genetics in Medicine* 17, no. 5: 405–424. https://doi.org/10.1038/gim.2015.30.

Riggs, E. R., E. F. Andersen, A. M. Cherry, et al. 2020. "Technical Standards for the Interpretation and Reporting of Constitutional Copy-Number Variants: A Joint Consensus Recommendation of the American College of Medical Genetics and Genomics (ACMG) and the Clinical Genome Resource (ClinGen)." *Genetics in Medicine* 22, no. 2: 245–257. https://doi.org/10.1038/s41436-019-0686-8.

Senger, B., D. L. Lafontaine, J. S. Graindorge, et al. 2001. "The Nucle(Ol)ar Tif6p and Efl1p Are Required for a Late Cytoplasmic Step of Ribosome Synthesis." *Molecular Cell* 8, no. 6: 1363–1373. https://doi.org/10.1016/s1097-2765(01)00403-8.

Stepensky, P., M. Chacón-Flores, K. H. Kim, et al. 2017. "Mutations in EFL1, an SBDS Partner, Are Associated With Infantile Pancytopenia, Exocrine Pancreatic Insufficiency and Skeletal Anomalies in a Shwachman-Diamond Like Syndrome." *Journal of Medical Genetics* 54, no. 8: 558–566. https://doi.org/10.1136/jmedgenet-2016-104366.

Tan, Q. K., H. Cope, R. C. Spillmann, et al. 2018. "Further Evidence for the Involvement of EFL1 in a Shwachman-Diamond-Like Syndrome and Expansion of the Phenotypic Features." *Cold Spring Harbor Molecular Case Studies* 4, no. 5: a003046. https://doi.org/10.1101/mcs.a003046.

Tan, S., L. Kermasson, A. Hoslin, et al. 2019. "EFL1 Mutations Impair eIF6 Release to Cause Shwachman-Diamond Syndrome." *Blood* 134, no. 3: 277–290. https://doi.org/10.1182/blood.2018893404.

Tummala, H., A. J. Walne, M. Williams, et al. 2016. "DNAJC21 Mutations Link a Cancer-Prone Bone Marrow Failure Syndrome to Corruption in 60S Ribosome Subunit Maturation." *American Journal of Human Genetics* 99, no. 1: 115–124. https://doi.org/10.1016/j.ajhg.2016.05.002.

Weis, F., E. Giudice, M. Churcher, et al. 2015. "Mechanism of eIF6 Release From the Nascent 60S Ribosomal Subunit." *Nature Structural & Molecular Biology* 22, no. 11: 914–919. https://doi.org/10.1038/nsmb.3112.

Zhu, B., Y. Guo, S. Lv, X. Ling, and S. You. 2024. "Hepatic Phenotypes of EFL1-Related Shwachman-Diamond Syndrome in a Biopsy-Validated Study." *Journal of Hepatology* 81, no. 3: e102–e104. https://doi.org/10.1016/j.jhep.2024.04.030.